

## A Comparative Evaluation of Welding Consumables for Dissimilar Welds between 310 Austenitic Stainless Steel and Inconel 657

H. Naffakh<sup>1</sup>, M. Shamanian<sup>2\*</sup> and F. Ashrafizadeh<sup>3</sup>

*Department of Materials Engineering, Isfahan University of Technology, Isfahan, 84156-83111, Iran*

---

### Abstract

The current work was carried out to characterize welding of AISI 310 austenitic stainless steel to Inconel 657 nickel-chromium superalloy. The welds were produced using four types of filler materials; the nickel-based corresponding to Inconel 82, Inconel A, Inconel 617 and austenitic stainless steels 310. Of the two joints involved, this paper describes the choice of welding consumables for the joint. The comparative evaluation was based on hot cracking tests (Varestraint test) and estimation of mechanical properties. While Inconel A exhibited the highest resistance to solidification cracking, the Inconel 617 filler material also showed moderate resistance and in addition, the latter was superior from the mechanical properties view-points. It was concluded that for the joint between Inconel 657 and 310 SS, the Inconel A filler material offered the best compromise.

*Keywords:* AISI 310, Inconel 657, Dissimilar Welding, Hot Cracking, Varestraint Test.

---

### 1. Introduction

One of the most important issues in the case of dissimilar welds is evaluation of proper filler materials for welds between Inconel 657 superalloy and 310 austenitic stainless steel. Superalloy Inconel 657 is widely used for high temperature applications in power and nuclear industries, which often involve joining by fusion welding. The alloy's weldability is generally considered not to be good in the autogenous or similar welding largely because of its HAZ and FZ cracking due to the precipitation kinetics of its principal precipitate  $\alpha$ -chromium in the FZ and HAZ<sup>1</sup>. In this condition, the alloy exhibits reasonably weak resistance to weld solidification cracking, and also it is prone to microfissuring in heat-affected zone (HAZ). Another concern is segregation of Nb and consequent formation of Nb-rich phase, a brittle compound, in the interdendritic regions during weld metal solidification. It is now well recognized that Nb-rich phase is detrimental to weldability and weld mechanical properties, particularly with respect to tensile ductility, fracture toughness, fatigue and creep rupture properties as it aids in easy crack initiation and propagation in addition to consuming significant amounts of useful alloying elements<sup>2</sup>. Presence of high content of chromium in the alloy composition leads to a decrease in heat conduction, therefore, heat concentration in the joint edges can cause cracking and distortion or localized melting. Also, presence of

delta ferrite in the autogenous welding of 310 stainless steel can improve solidification cracking of the weld metal. Also fine dendritic structure of weld in this steel enhances the fracture toughness and ductility. It is well-known that austenitic welds which have 4-10 vol% delta ferrite and fine dendrites can resist the hot cracking, stresses and severe impacts under service<sup>3</sup>.

In oil-converter towers, the temperature can reach 1050°C and the atmosphere is too carburizing and oxidizing<sup>4,5</sup>; thus, Inconel 657 alloy as heat-flow controlling components (dampers) and supports (hangers) in the reformer towers, is a suitable choice. The rotating axles which control the damper motion, are made of 310 SS because it is exposed to lighter atmosphere and lower temperature. To join the dampers to the axles located in the wall tower, fusion welding is the normal process. Nevertheless, for such dissimilar joints, it appears that the type of proper filler material, physical and mechanical properties of the weld and weldability have not been sufficiently studied and the published work is very limited. This study was performed to investigate the most appropriate filler material based on a comparative evaluation of the four consumables in weldability and mechanical properties of the welds.

### 2. Experimental work

The base materials used in this study were 12 mm thick plates of 310 steel and Inconel 657, the former was solution-annealed and the latter was in the as-cast condition. The four consumables examined were Inconel 82 (gas tungsten arc filler

---

\* Corresponding author:

Tel: +98- 311- 3915737 Fax: +98- 311- 3912752

E-mail: shamanian@cc.iut.ac.ir

Address: Dept. of Materials Engineering, Isfahan University of Technology, Isfahan, 84156-83111, Iran

---

1. M.Sc Student  
2. Associate Professor  
3. Professor

wires), Inconel A, Inconel 617 and 310 stainless steel (manual metal arc electrodes). The nominal chemical compositions of the base materials and the filler materials are given in Table 1. Also, welding parameters are presented in Table 2. Material optimization was based on tests for evaluation of hot cracking susceptibility, tensile properties, hardness and notch toughness. Hot cracking was studied by longitudinal Varestraint test for comparing the filler rods. Prior to Varestraint testing, welded joints were made between the base materials using each of the four filler materials, employing a V groove edge with an included angle of 75° and 2.5 mm root opening gap and 1mm root face.

The welded sections were sliced and machined into strips, with the weld metal located along the pieces at the centre. Laboratory scale specimens of dimensions 150×25×3.2 mm<sup>3</sup> were then prepared for Varestraint testing. Hot cracking susceptibility of the weld metals was tested on a moving torch Varestraint hot cracking test device. During the test, an autogeneous gas tungsten-arc weld bead was deposited on the original weld metal and solidification cracking was induced by applying a predetermined bending strain through a pneumatically activated ram forcing the sample to conform to the radius of a die block. The augmented bending strain  $e$  applied to the surface of the test

Table 1- Nominal chemical composition of materials used (wt %)

| Elements | Base metals |             |            | Filler materials |           |         |
|----------|-------------|-------------|------------|------------------|-----------|---------|
|          | 310 SS      | Inconel 657 | Inconel 82 | Inconel 617      | Inconel A | 310 SS  |
| C        | Max 0.1     | Max 0.2     | Max 0.1    | Max 0.1          | Max 0.1   | Max 0.1 |
| Si       | 1           | 1           | 0.5        | 1                | 1         | 1       |
| Mn       | 2           | 1           | 3          | 2                | 3         | 2       |
| Fe       | Rem.        | 1           | 3          | 5.5              | 12        | Rem.    |
| Cr       | 26          | 45          | 20         | 25               | 15        | 26      |
| Mo       | -           | -           | -          | 10               | 1.5       | -       |
| Co       | -           | -           | -          | 10               | -         | -       |
| Ti       | -           | -           | 1          | 0.6              | -         | -       |
| Nb       | -           | 1           | 3          | 1                | 2.5       | -       |
| Al       | -           | -           | -          | 1                | -         | -       |
| Ni       | 21          | Rem.        | Rem.       | Rem.             | Rem.      | 21      |
| Cu       | -           | -           | 0.5        | 0.5              | 0.5       | 0.75    |

Table 2. Parameters of welding

| Filler materials | Welding process | Pass number | current (A) | voltage (V) | Welding speed (mm/s) | Heat input (KJ/mm) | Total heat input (KJ/mm) |
|------------------|-----------------|-------------|-------------|-------------|----------------------|--------------------|--------------------------|
| Inconel 82       | GTAW            | 1           | 120         | 12          | 1                    | 1.44               | 5.93                     |
|                  | GTAW            | 2           | 110         | 12          | 1.1                  | 1.2                |                          |
|                  | GTAW            | 3           | 110         | 14          | 0.85                 | 1.81               |                          |
|                  | GTAW            | 4           | 105         | 12          | 0.85                 | 1.48               |                          |
| Inconel A        | GTAW            | 1           | 135         | 12          | 0.77                 | 2.10               | 8.94                     |
|                  | SMAW            | 2           | 105         | 26          | 1.76                 | 1.55               |                          |
|                  | SMAW            | 3           | 105         | 24          | 1.43                 | 1.76               |                          |
|                  | SMAW            | 4           | 105         | 24          | 1.25                 | 2.02               |                          |
|                  | SMAW            | 5           | 105         | 24          | 1.67                 | 1.51               |                          |
| Inconel 617      | GTAW            | 1           | 130         | 12          | 1.20                 | 1.30               | 7.19                     |
|                  | SMAW            | 2           | 90          | 24          | 1.58                 | 1.37               |                          |
|                  | SMAW            | 3           | 110         | 24          | 1.15                 | 2.30               |                          |
|                  | SMAW            | 4           | 120         | 24          | 1.30                 | 2.22               |                          |
| 310 SS           | GTAW            | 1           | 130         | 12          | 1                    | 1.56               | 6.49                     |
|                  | SMAW            | 2           | 100         | 25          | 3                    | .83                |                          |
|                  | SMAW            | 3           | 110         | 25          | 1.88                 | 1.33               |                          |
|                  | SMAW            | 4           | 110         | 25          | 1.76                 | 1.56               |                          |
|                  | SMAW            | 5           | 110         | 22          | 2                    | 1.21               |                          |

specimen is related to the radius of the die block by the equation  $e = t/2R$ , where  $t$  is the specimen thickness and  $R$  is the radius of the die block. The strain levels applied were 1%, 2% and 4%. The welding parameters used during Varcstraint testing were kept constant as follows: current = 130 A, voltage = 18 V and travel speed = 4.5 mm/s. Following the test procedure, the specimens were examined at a magnification of 50 using a stereomicroscope for measuring crack length. Both total crack length (TCL) and maximum crack length (MCL) were used as criteria for evaluating the hot cracking susceptibility of the weld metals.

Transverse sections of the welds were metallographically characterized after etching in marble solution (10gr CuSO<sub>4</sub> + 50 mlit HCl + 50mlit H<sub>2</sub>O). The weldments were examined by optical and scanning electron microscopy using standard metallographical techniques. Chemical compositions were determined by energy dispersive X-ray spectrometer (EDS) using Oxford Cam Scan MV2300. Transverse tensile specimens (length perpendicular to welding direction) were produced and tested at room temperature according to AWS B4 standard with 28.6 mm gauge length and 4 mm gauge diameter using Hounsfield H50KS tester. The samples were tested at a nominal strain rate of 1.2 mm/min at room temperature. Microhardness measurements were made across the weld metals at a load of 100 g using a Leitz microhardness tester. Room-temperature toughness of the welds was

determined by standard 55×10<sup>3</sup> mm<sup>3</sup> Charpy V-notch impact specimens using Amsler tester. The fracture faces were examined on a Philips scanning electron microscope.

### 3. Results and discussion

#### 3. 1. Microstructures

Figure 1 a,b display the fusion zone microstructure of Inconel 82 weld metal. It can be seen that microstructure is fully austenitic, indicating lack of allotropic transformation during cooling. This weld metal contains 3 percent niobium. Cieslak and Dupont indicated that Nb has a high tendency to increase the bulk solidification temperature range. In other words, it increases the degree of constitutional undercooling, causing this region to widen<sup>6-8</sup>. Thus, the substructure tends to change from cellular to columnar dendritic, as the degree of constitutional undercooling is increased. The Nb content in the Inconel 82 weld is sufficient to change the FZ solidification mode and could pin grain boundaries, thus hindering growth. It is seen that continuous NbC (shiny precipitates) and distributed TiC precipitates (dark particles) are formed in the interdendritic regions. Based on these micrographs, there is no clear evidence on the formation of lamellar  $\gamma$ /laves eutectic in the interdendritic regions. This weld metal did not show formation of other second phases (such as Topologically Closed Phases), either.

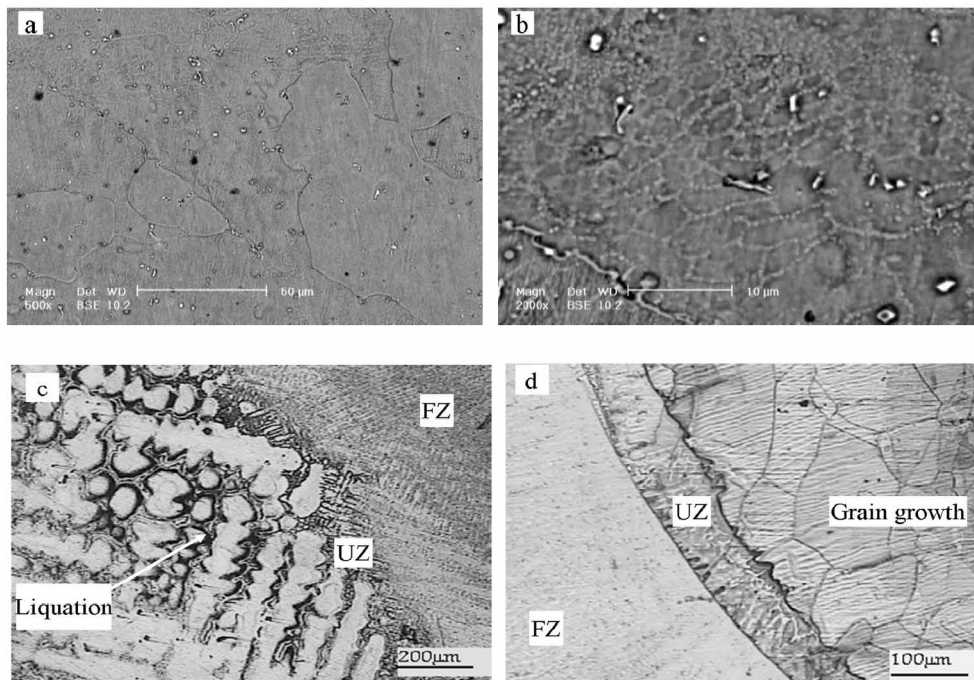


Fig. 1. Weld metal made with Inconel 82 filler metal: (a) interior of weld, (b) interior of weld in higher magnification, (c) interface with Inconel 657 base metal and (d) interface with 310 SS base metal.

The interface between Inconel 82 weld metal and Inconel 657 base metal is shown in Figure 1c. The unmixed zone exists as a laminar layer where a small portion of the base metal has completely melted and resolidified without undergoing filler metal dilution. The microstructure of the interface heat-affected zone shows extensive grain boundary melting and liquation. The partially melted zone on this side of the joint appears to be wider than that on other side (Figure 1d). The tendency of dendritic boundaries to melt in alloy Inconel 657 is attributed to the enrichment of niobium at these boundaries. Niobium not only lowers the melting point constitutionally, but also forms low melting carbide-austenite eutectics during solidification.

Figures 2 a,b exhibit fusion zone of Inconel A weld metal. Although Inconel A, similar to Inconel 82, has considerable amount of niobium (2.5 percent), its iron content (12 percent) is much more than Inconel 82 (3 percent). Presence of iron in nickel-based superalloys lowers the niobium solubility in austenite phase. With iron in the nickel-chromium solid solution, the ability of Nb to remain in solution is limited<sup>6)</sup> and partitioning of Nb to the interdendritic regions in the weld metal is enhanced.

Segregation of alloying elements caused broadening of the brittleness temperature range (BTR) and constitutional supercooling. Presence of higher content of nickel and less amount of chromium in Inconel A weld metal than that of Inconel 82 can lead to dissolve superior niobium percent in Inconel A austenite, and therefore the formation of low melting phases in the intergranular regions decreases. It can be predicted that hot cracking resistance of Inconel A is more than Inconel 82 weld metal. The interface of Inconel A weld metal with Inconel 657 base metal (Fig. 2c) as well as Inconel 82 weld metal (Figure 1c) shows the presence of an unmixed zone.

Figure 3a shows the fusion zone microstructure of Inconel 617 filler material. The Mo partition coefficient decreases as the iron content in the weld increases (i.e., as the dilution level is increased). The SEM micrograph in Fig. 3b shows that the microstructure of Inconel 617 weld metal consists of columnar dendrites as a result of strong Mo constitutional under cooling effect. This structure seems to be coarser than Inconel 82 and Inconel A weld metals. It is well-known that coarse-dendritic structures have more tendency to solidification cracking<sup>6-11)</sup>.

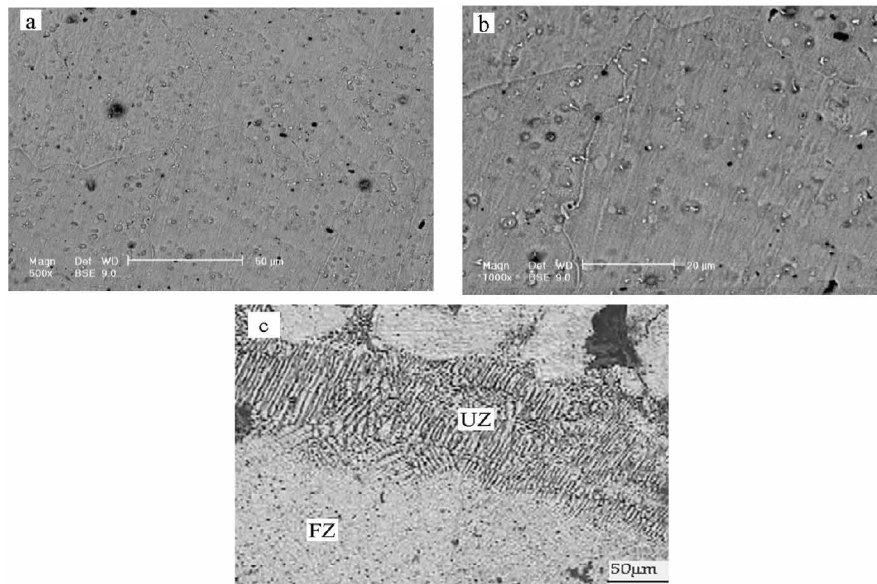


Fig. 2. Weld metal with Inconel A filler metal: (a) interior of weld, (b) interior of weld in higher magnification, (c) interface with Inconel 657 base metal.

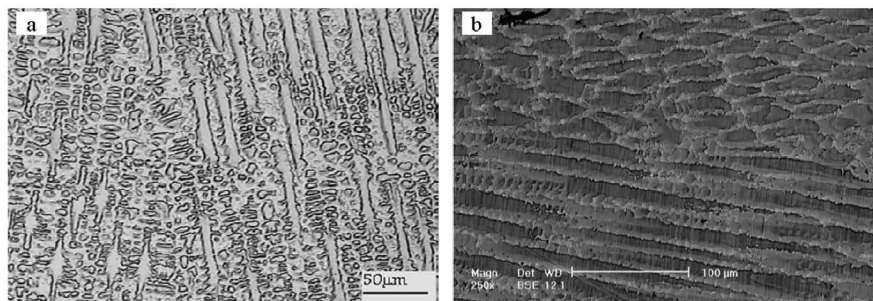


Fig. 3. Weld metal with Inconel 617 filler metal (a) interior of weld, (b) SEM photograph of weld metal.

Figure 4a illustrates cellular structure in the 310 SS fusion zone. Since the weld metal contains some copper, formation of secondary phases which make weld metal more prone to hot cracking is probable (Fig. 4b). A large number of secondary phases and globular precipitates are formed in the matrix. Also oxide inclusions are distributed interior of weld metal. Figure 4c shows the magnified view of partially melted zone and unmixed zone in Inconel 657 interface attributed to 310 SS weld metal. On the other side of joint, the interface between 310 SS weld metal and 310 SS base metal has been shown in Figure 4d. The microstructure reveals ferrite stringers in some of the austenite grains in the base metal close to the HAZ. It can be observed that type I boundaries has formed in the weld metal (Figure 4d). In the current work all micrographs of the interface regions show that only type I boundaries are present.

### 3.2. Hardness survey

Variations of hardness across the welds are shown in Figure 5. The welds possessed hardness values higher than those of the 310 base metal and lower than Inconel 657 in all cases. It should also be noticed that in all cases there is a gradual, though slight, increase in hardness in the weld metal on traversing from 310 steel to Inconel 657 side. This suggests that despite the convection effects in the weld metal, there is a composition gradient on account of dilution from two different base materials. The weld metals show great differences in the average hardness. Inconel A weld metal exhibits the highest hardness value among the weld metals studied, whereas 310 SS weld metal displays the lowest value. This big difference is attributed to the chemical composition of the filler rods. Inconel 82 and Inconel A have more solid solution strength than 310 SS.

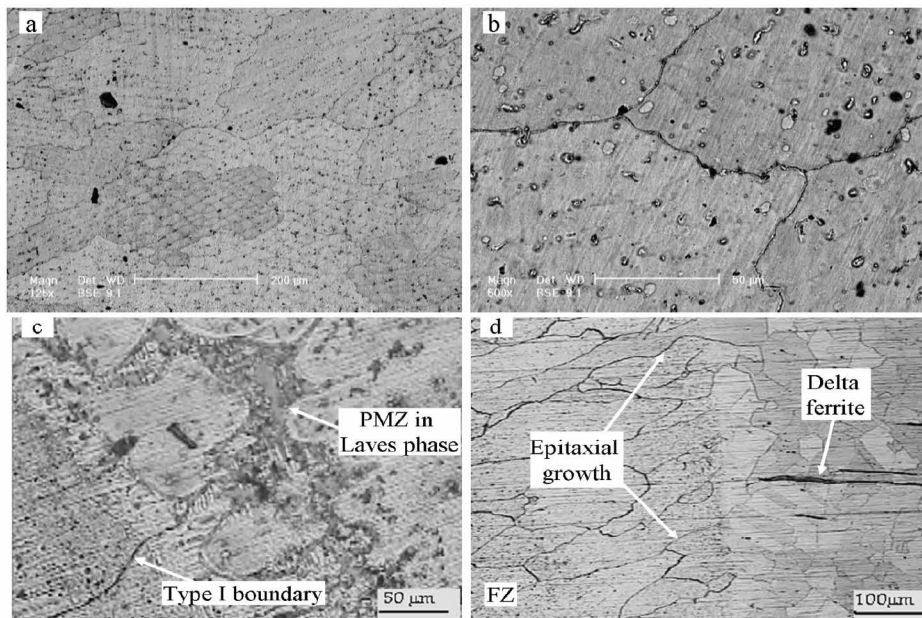


Fig. 4. Weld metal made with 310 SS filler metal: (a) interior of weld, (b) interior of weld in higher magnification, (c) interface with Inconel 657 base metal, and (d) interface with 310 SS base metal.

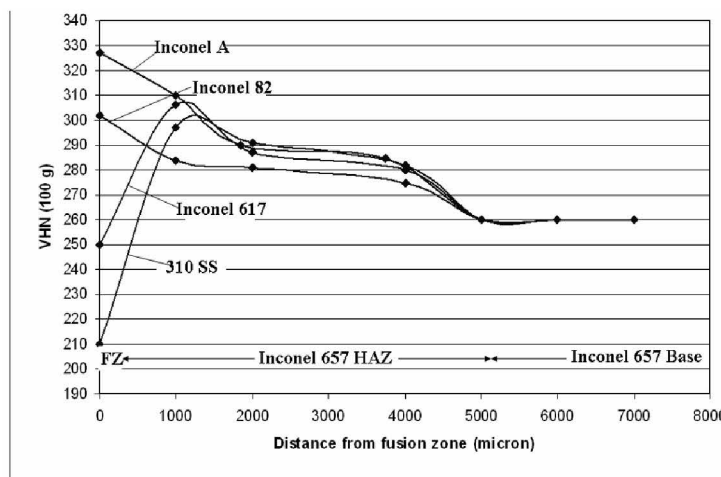


Fig. 5. Hardness profile across the welds produced with different fillers.

In addition,  $\alpha$ -Cr precipitation of Inconel 657 in the heat affected zone has occurred. Inconel 657 base metal has a metastable structure and can transform to chromium enriched structure under sufficient temperature and time to produce a stable condition<sup>1)</sup>. In this study, Inconel 657 base metal of all investigated weldments showed  $\alpha$ -Cr precipitates in the heat affected zone. Figure 6 displays the  $\alpha$ -Cr precipitation regions in the Inconel 657 HAZ. It can be seen that the hardness increased from weld metal to HAZ in the case of weld metals; a good evidence for this phenomenon. This phenomenon can cause improving the mechanical properties and decreasing the hot oxidation resistance at elevated temperatures<sup>1,4)</sup>.

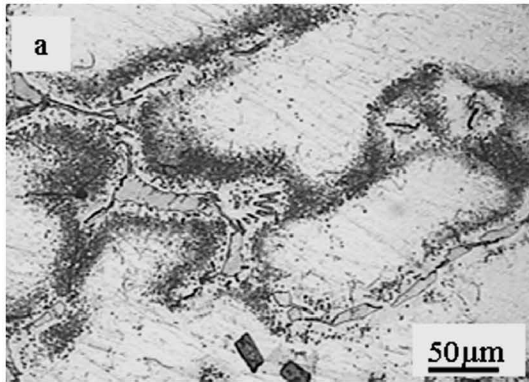


Fig. 6. Precipitation in Inconel 657 HAZ.

### 3.3. Hot cracking susceptibility

The results of the longitudinal Varestraint testing in Figure 7 show the dependence of total crack length and maximum crack length, respectively, on the applied strain. It is clear from the diagrams that Inconel A weld metal has the least susceptibility to hot cracking. Inconel A weld metal contains a considerable amount of niobium, silicon and chromium and is prone to hot cracking. Based on Figures 2a, b, it can be seen that there isn't any continuous network of low melting phases in interdendritic or intergranular regions. The occasional anomalous behaviour observed in some cases may be attributed to the preparation procedure of specimens. While in the conventional Varestraint testing, wrought base metal specimens are directly used. In the current investigation weld metals were first produced using the filler materials and the remelted during the Varestraint testing. Minor variations in dilution at the region of strain application might have caused the observed behaviour<sup>12-14)</sup>.

In Fig. 7a, it is noticed that weld metals, except Inconel 82, show no cracking at 1% strain, thus signifying the threshold strain. Total crack length in Inconel 82 and Inconel 617 does not change when the strain is increased from 2% to 4%, thus, revealing a saturation effect at 2% strain. It is also observed in Fig. 7b that the maximum crack length for Inconel A

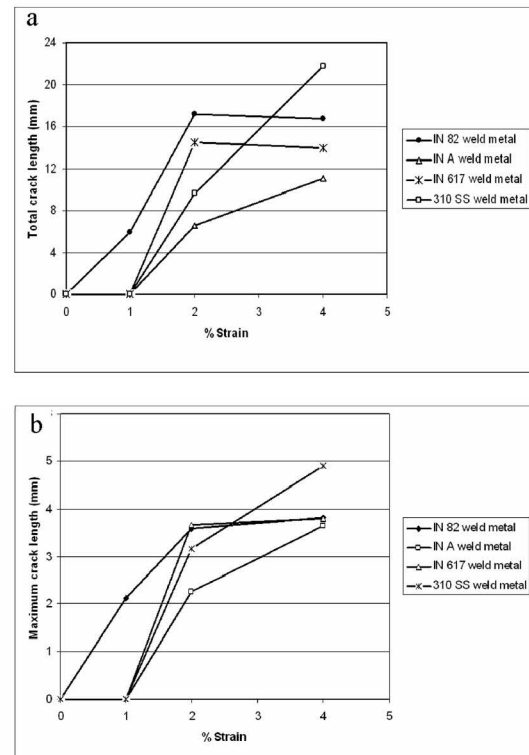


Fig. 7. Varestraint testing results: (a) Total crack length in fusion zone for the four weld metals, (b) maximum crack length in fusion zone for the four weld metals.

weld metal is the least value at all applied strains. According to these results, Inconel 82 shows a higher tendency to solidification cracking than other filler materials, which is in agreement with previous investigations<sup>8,10)</sup>. On the other hand, 310 SS filler metal shows low resistance to hot cracking. Presence of low melting phases enriched in Cu, located continuously in the intergranular locations, is the most important factor to widening BTR and solidification cracking. The welds had no crater cracking except 310 SS weld metal which displayed crater cracks at all the applied stresses. Optical micrographs of the cracked regions are shown in Fig. 8a-f. The cracking appears to be predominantly intergranular, and some cracks lie along the substructure boundaries. Extensive cracking in the weld metals is probably a result of predominantly austenitic mode of solidification and pronounced dendritic morphology. Many cracks exhibited backfilling as shown by arrows in Figures 8a, b and c.

Results of energy dispersive spectroscopy are presented in Fig. 9a-f and Table 3 for rich phases located at crack ends. In the case of Inconel 82 and Inconel A weld metals, presence of niobium, sulfur and copper is the most important factor influencing the formation of low melting phases in the interdendritic and intergranular regions. On the other hand, for Inconel 617 weld metal, presence of copper, aluminum and titanium caused formation of phases susceptible to solidification cracking.

Presence of Cu in the enriched low melting phases, and therefore its detrimental effect on the current 310

SS weld metal is in opposition to previous investigates<sup>12)</sup>.

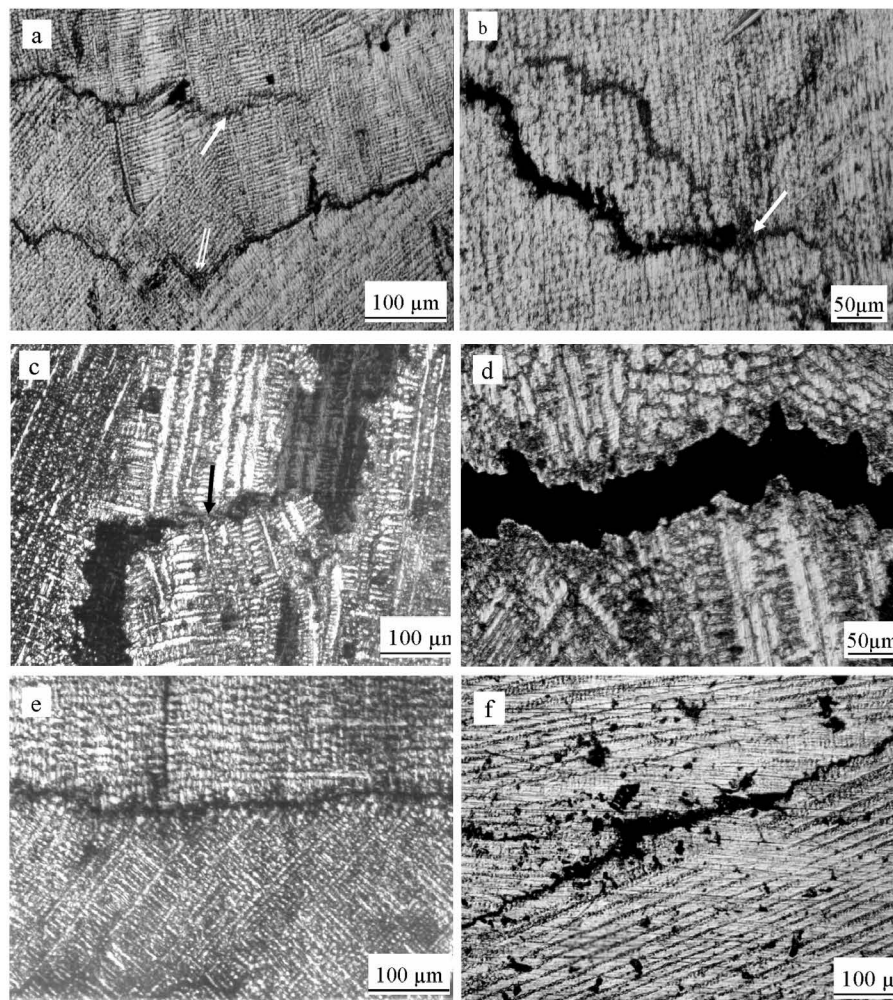


Fig. 8. (a) Solidification cracking in Inconel 82 weld metal showing back-filled region (arrow), (b) the same as Fig. 8a showing back-filled region (arrow) in higher magnification, (c) solidification cracking in Inconel 617 weld metal showing back-filled region (arrow), (d) the same as Fig. 8c in higher magnification (e) solidification cracking in Inconel A weld metal, and (f) solidification cracking in 310 SS weld metal.

Table 3. EDS values for Figs. 9a-f

| Alloying Elements | (a)  | (b)  | (c)  | (d)  | (e)  | (f)  |
|-------------------|------|------|------|------|------|------|
| Si K $\alpha$     | 0.7  | -    | 1.6  | -    | -    | -    |
| Cr K $\alpha$     | 35.4 | 8.4  | 14.3 | 39.9 | 4.6  | 25.8 |
| Mn K $\alpha$     | 3.1  | 1.3  | 0.9  | 2.9  | -    | 1.9  |
| Fe K $\alpha$     | 3.9  | 25.8 | 6.6  | 6.5  | 1.6  | 35.5 |
| Ni K $\alpha$     | 34.8 | 41.9 | 44.8 | 23.6 | 20.7 | 19.3 |
| Nb K $\alpha$     | 22.2 | -    | 29.9 | -    | -    | -    |
| S K $\alpha$      | -    | 5.7  | 1.9  | 1.5  | -    | 1.3  |
| Cu K $\alpha$     | -    | 16.8 | -    | -    | 65.5 | 16.1 |
| Al K $\alpha$     | -    | -    | -    | 5.8  | -    | -    |
| Ti K $\alpha$     | -    | -    | -    | 15.1 | -    | -    |
| Co K $\alpha$     | -    | -    | -    | 4.8  | -    | -    |

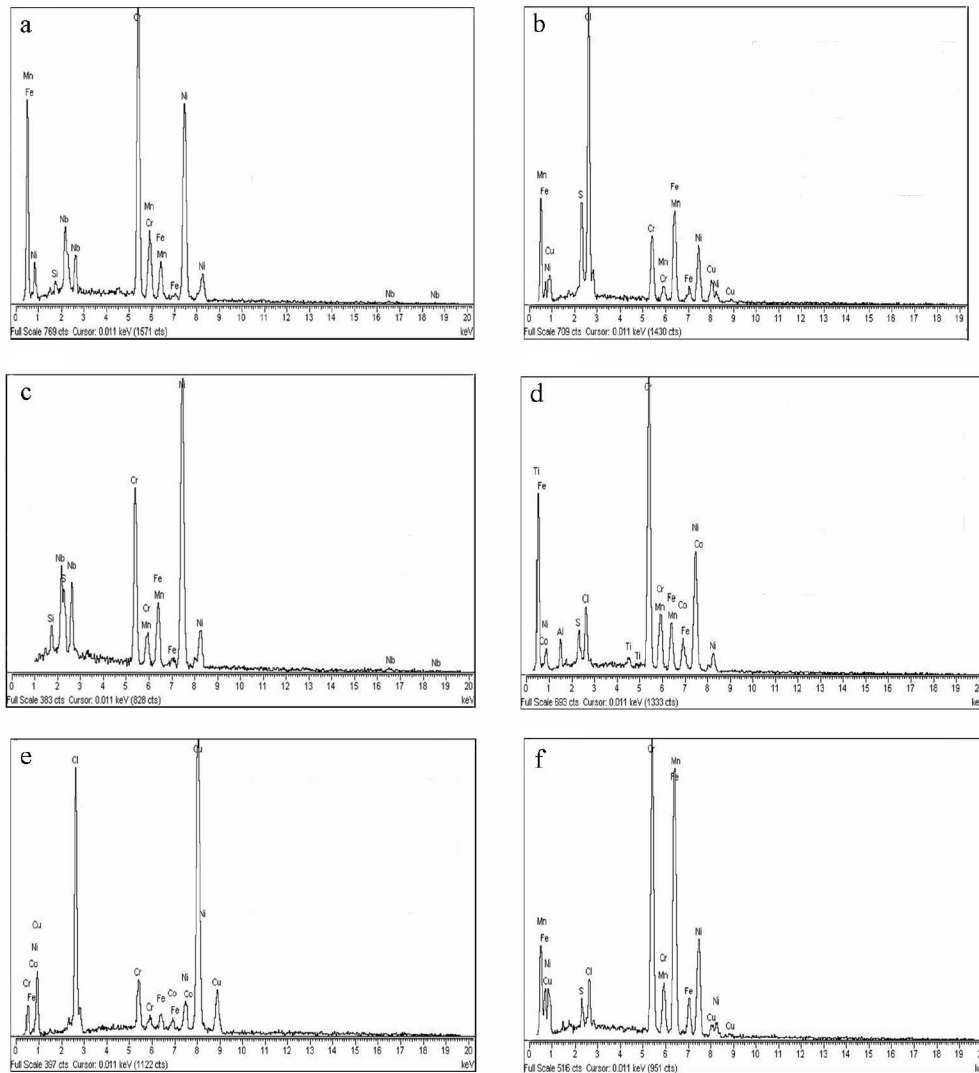


Fig. 9. EDS results for (a) Nb rich phase In Inconel 82 weld metal, (b) Cu and S rich phase In Inconel A weld metal, (c) Nb rich phase In Inconel A weld metal, (d) Al and Ti rich phase In Inconel 617 weld metal, (e) Cu rich phase In Inconel 617 weld metal and (f) Cu rich phase In 310 SS weld metal.

### 3.4. Tensile properties

Typical stress-strain curves obtained at room temperature are shown in Figures 10a-d. During the transverse tensile tests, all weldments failed at the weaker parent metal, i.e., within Inconel 657. As mentioned before, Inconel 657 base metal had a coarse, fully dendritic microstructure leading to low fracture toughness. Thus, fracture of metal took place before experiencing a considerable amount of ductile elongation. Presence of many micro- and macro-fissures in the gage length towards Inconel 657 section, reveals the high level of metal solidification shrinkages. The most significant result from these tests is that Inconel A weldment had the highest value of strength and total elongation. Comparison between these results, according to Fig. 10a-d, shows that uniform plastic deformation of Inconel A weld metal helps Inconel 657 base metal to bear higher

stresses. This is attributed to the high percentage of nickel in the chemical composition of Inconel A. In contrast, Inconel 82 shows the lowest ultimate strength. It is known that this alloy has good toughness, but high work hardening ratio caused Inconel 82 weld metal to limit plastic deformation at the low level of stresses. Under these conditions, Inconel 657 base metal ruptures before the weld metal could complete its uniform elongation. On the other hand, Inconel 617 weld metal exhibits the lowest total elongation among the four experimented weld metals. It can be attributed to high molybdenum segregation in the weld metal boundaries that enhanced weld metal embrittlement.

### 3.5. Notch toughness

The Charpy test results for as-welded specimens are listed in Table 4. The base metal toughness



values are included for comparison, too. In addition, the fracture surfaces of the weld metal specimens after Charpy tests were examined by the scanning electron microscope and the fractographs are presented in Figure 11a-f. Microstructure of Inconel 657 is composed of dendrites that tend to be very brittle and the fractographs exhibit regions of cleavage fracture. In contrast, 310 base metal has a very tough structure that can be attributed to ductile annealed austenitic phase. Fracture surface of this base metal is composed of deep dimples which reveal high resistance to fracture. The weld metals show

fully ductile rupture except Inconel 617 which exhibits mixed fracture. It can be seen that the fracture surface is composed of regions of cleavage fracture and plastic deformation. The Charpy V - notch impact energies at room temperature for the four filler metals exceed the impact energy of Inconel 657 base metal and, therefore, all weldments can resist unpredicted impacts under service conditions if the Inconel 657 doesn't fail by brittle fracture. Inconel 617 is more critical because this weld metal had the lowest toughness value.

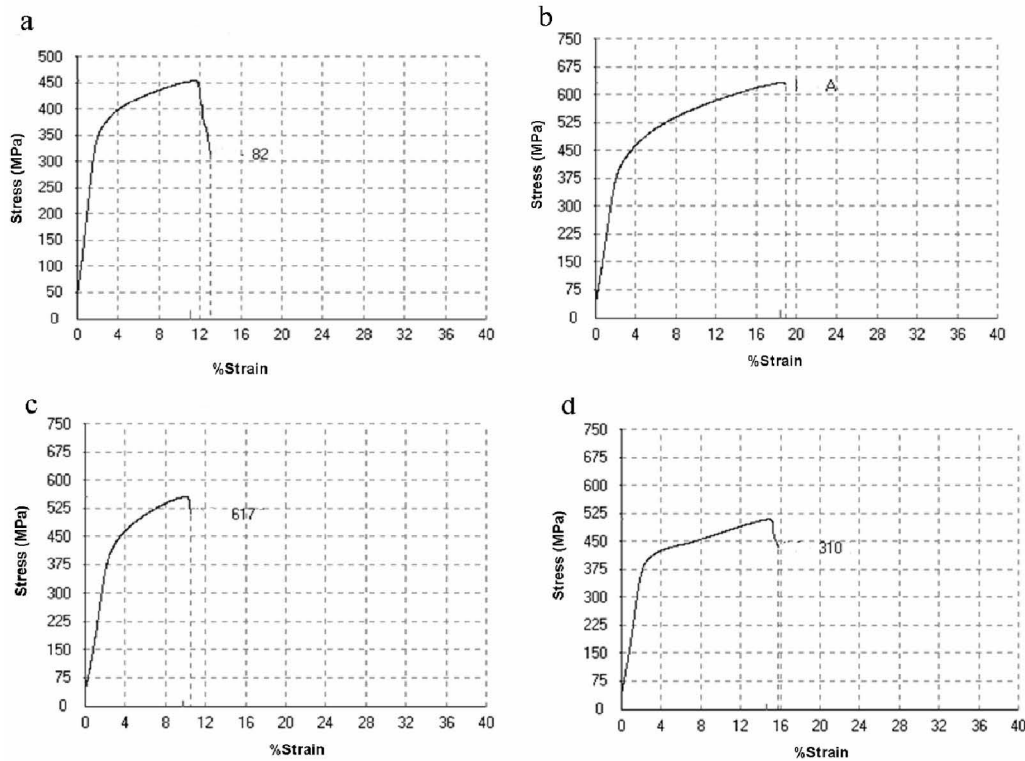


Fig. 10. Tensile curves of transverse specimens at room temperature for; (a) Inconel 82 weldment, (b) Inconel A weldment, (c) Inconel 617 weldment and (d) 310 SS weldment.

Table 4. Charpy V-notch impact energy at room temperature

| Material                              | Impact energy (J) | Type of fracture |
|---------------------------------------|-------------------|------------------|
| Inconel 657 (base metal)              | 13                | fully brittle    |
| Type 310 stainless steel (base metal) | 217               | fully ductile    |
| Inconel 82 weld metal                 | 121               | fully ductile    |
| Inconel A weld metal                  | 100               | fully ductile    |
| Inconel 617 weld metal                | 51                | ductile-brittle  |
| 310 SS weld metal                     | 100               | fully ductile    |

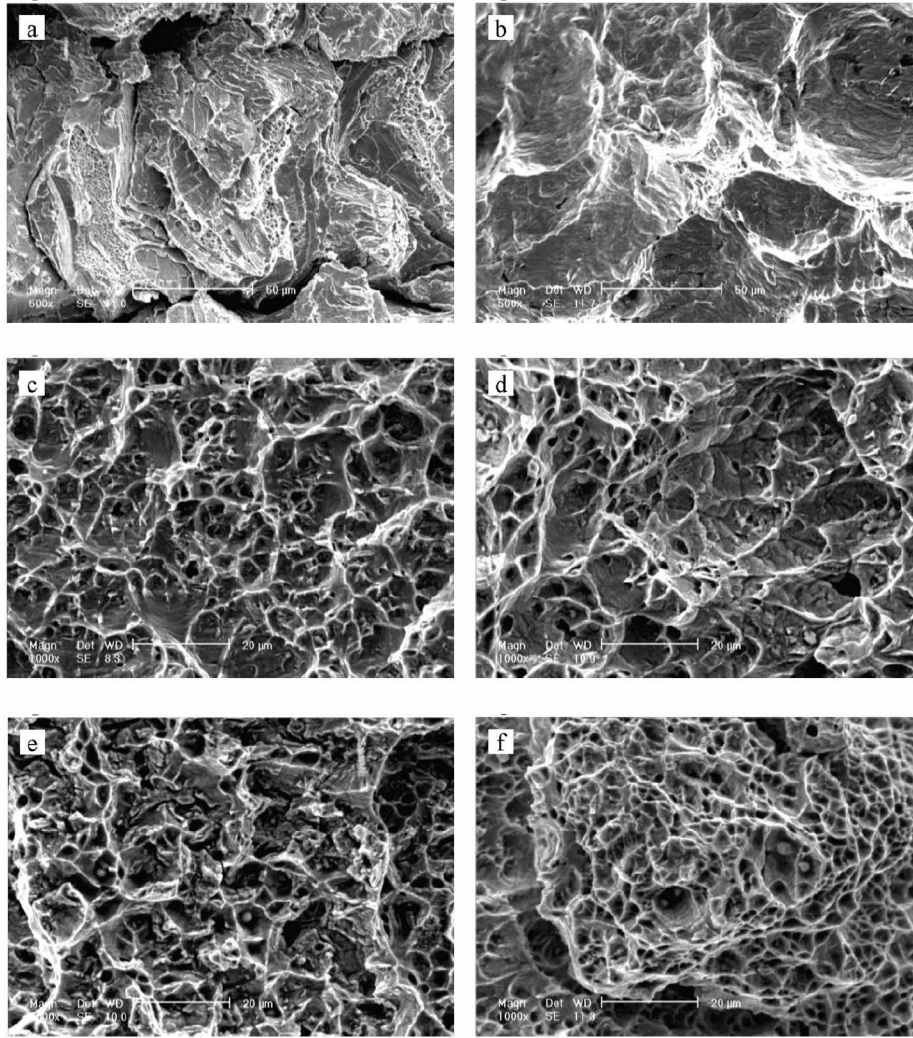


Fig. 11. SEM fractographs of fractured Charpy impact specimens: (a) Inconel 657 base metal, (b) 310 SS base metal, (c) Inconel 82 weld metal, (d) Inconel A weld metal, (e) Inconel 617 weld metal and (f) 310 SS weld metal.

#### 4. Conclusions

1- All weld metals have fully-austenitic microstructures.  $\gamma$ /NbC eutectic structure and TiC precipitates were formed in the interdendritic regions of Inconel A and Inconel 82 weld metals. Inconel 617 weld metal displayed coarser dendritic structure in comparison to Inconel 82 and Inconel A weld metal. 310 SS weld metal microstructure consisted of cellular structure and continuous networks in the boundaries.

2- Unmixed zone, partially melted zone and heat affected zone on both sides of joints were formed. Inconel 657 base metal had UZ and PMZ, but in 310 SS base metal, a significant PMZ was not observed.

3- Inconel A weld metal had the highest hardness value, whereas Inconel 82 displayed the lowest value. A-Cr precipitation of Inconel 657 in the heat affected

zone has occurred.

4- According to Vareststraint tests, Inconel A had the least susceptibility to hot cracking. Inconel 82 and 310 SS weld metals showed higher tendency to solidification cracking. EDS results showed formation of rich phases in segregants located in the end of cracks.

5- In tension tests, all weldments failed in the weaker parent metals, i.e., Inconel 657. Inconel A weldment had the highest strength and total elongation whereas Inconel 82 displayed the lowest strength.

6- The weld metals failed by ductile rupture except Inconel 617 which exhibited a mixed fracture mode.

7- It can be concluded that for joints between 310 stainless steel and Inconel 657 base metal, Inconel A filler material offers optimum properties at room temperature.

## References

- [1] G. Belloni, G. Caironi, A. Gariboldi, A. Lo Conte Politecnico di Milano, Washington DC, August 2001 Paper 1546 Trans.
- [2] E. Gariboldi, G. Caironi Representation Proc. of 61th World Foundry Cong., Beijing, China, 1995.
- [3] R. Kacar, O. Baylan, Mater. Design 25(2004), 317.
- [4] Li Jian, C. Y. Yuh, M. Farooque, Corros. Sci. 42(2000), 1573.
- [5] Shuangqun Zhao, b. Xishan Xie, Gaylord D. Smith, Surf. Coat. Technol. 185(2004), 178.
- [6] J. N. Dupont, S. W. Banovic, A. R. Marder, Weld. J., 82(2003), 125s.
- [7] H. T. Lee, S. L. Jeng, C. H. Yen, T. Y. Kuo, J. Nucl. Mater. 335(2004), 59.
- [8] Tsung-Yuan Kuo, Hwa-Teng Lee, Mater. Sci. Eng. A, 338(2002), 202.
- [9] M. Sireesha, V. Shankar, Shaju K. Albert, S. Sundaresan, Mater. Sci. Eng. A, 292(2000), 74.
- [10] M. Sireesha, Shaju K. Albert, V. Shankar, S. Sundaresan, J. Nucl. Mater., 279(2000), 65.
- [11] N. Wang, S. Mokadem, M. Rappaz W. Kurz, Acta Mater., 52(2004), 3173.
- [12] M. D. Rowe, P. Crook, G. L. Hoback, Weld. J., 82(2003), 313.
- [13] W. F. Savage, C. D. Lundin, Weld. J., 45(1966), 497s.
- [14] W. F. Savage, C. D. Lundin, Weld. J., 44(1965), 433.